

Nucleon Structure in Lattice QCD using twisted mass fermions

C. Alexandrou* ^(a,b), **M. Constantinou** ^(a), **T Korzec** ^(a,c),

^(a) *Department of Physics, University of Cyprus, P.O. Box 20537, 1678 Nicosia, Cyprus*

^(b) *Computation-based Science and Technology Research Center, Cyprus Institute, 20 Kavafi Str., Nicosia 2121, Cyprus*

^(c) *Institut für Physik Humboldt Universität zu Berlin, Newtonstrasse 15, 12489 Berlin, Germany*

E-mail: alexand@ucy.ac.cy, constantinou.martha@ucy.ac.cy,

korzec@physik.hu-berlin.de

J. Carbonell, P. A. Harraud, M. Papinutto

Laboratoire de Physique Subatomique et Cosmologie, UJF/CNRS/IN2P3, 53 avenue des Martyrs, 38026 Grenoble, France

E-mail: Jaume.Carbonell@lpsc.in2p3.fr, harraud@lpsc.in2p3.fr,

Mauro.Papinutto@lpsc.in2p3.fr

P. Guichon

CEA-Saclay, IRFU/SPhN, 91191 Gif-sur-Yvette, France

E-mail: pierre.guichon@cea.fr

K. Jansen

NIC, DESY, Platanenallee 6, D-15738 Zeuthen, Germany

E-mail: Karl.Jansen@desy.de

We present results on the nucleon form factors and moments of generalized parton distributions obtained within the twisted mass formulation of lattice QCD. We include a discussion of lattice artifacts by examining results at different volumes and lattice spacings. We compare our results with those obtained using different discretization schemes and to experiment.

*35th International Conference of High Energy Physics - ICHEP2010,
July 22-28, 2010
Paris France*

*Speaker.

1. Introduction

Lattice QCD simulations are currently being performed with two dynamical degenerate light quarks with a mass close to their physical value as well as the strange quark using a number of different discretization schemes with the most common being Wilson-improved, staggered and chiral fermions. Furthermore, simulations at several lattice spacings and volumes are becoming available enabling a comprehensive study of lattice artifacts.

The focus of this contribution is the evaluation of form factors (FFs) and moments of parton distributions of the nucleon, which are being measured in many experiments. The characterization of nucleon structure is considered a milestone in hadronic physics and experiments on nucleon FFs started in the 50s. A new generation of experiments using polarized beams and targets are yielding high precision data spanning a larger range of momentum transfers. FFs provide ideal probes of the charge and magnetization densities of the hadron as well as a determination of its shape.

Lattice techniques to extract nucleon matrix elements connected to FFs and moments of generalized parton distributions (GPDs) are well developed. The connected diagram where an operator couples to a valence quark is straightforward to compute and has been evaluated by a number of lattice groups [1]. For iso-vector nucleon matrix elements, in the isospin limit, this is the only contribution. Like most collaborations, we use non-perturbative renormalization of these matrix elements and furthermore we subtract $\mathcal{O}(a^2)$ -terms computed perturbatively to improve the extraction of the renormalization constants [2]. Using simulations of $N_F = 2$ twisted mass fermions (TMF) at three values of the lattice spacing and different volumes we study cut-off and volume effects. We use the lattice spacing determined from the nucleon mass to convert to physical units. Heavy baryon chiral perturbation theory (HB χ PT) is used to extrapolate lattice results obtained for pion masses in the range of about 260 MeV to 470 MeV to the physical point.

2. Nucleon form factors

The nucleon matrix element of the electromagnetic (EM) current, $j_\mu = \bar{\psi}(x)\gamma_\mu\psi(x)$, is written in the form $\bar{u}_N(p', s') \left[\gamma_\mu F_1(q^2) + \frac{i\sigma_{\mu\nu}q^\nu}{2m} F_2(q^2) \right] u_N(p, s)$, where the Dirac F_1 and Pauli F_2 FFs are related to the electric and magnetic Sachs FFs with the relations: $G_E(q^2) = F_1(q^2) - \frac{q^2}{(2m)^2} F_2(q^2)$ and $G_M(q^2) = F_1(q^2) + F_2(q^2)$. For the axial vector current, $A_\mu^a = \bar{\psi}(x)\gamma_\mu\gamma_5\frac{\tau^a}{2}\psi(x)$, the nucleon matrix element is of the form $\bar{u}_N(p', s') \left[\gamma_\mu\gamma_5 G_A(q^2) + \frac{q^\mu\gamma_5}{2m} G_P(q^2) \right] \frac{1}{2}u_N(p, s)$.

The axial charge is well known experimentally. Since it is determined at $Q^2 = 0$ there is no ambiguity associated with fitting the Q^2 -dependence of the FF. As can be seen in Fig. 1, where we show recent lattice results using TMF, domain wall fermions (DWF) and a hybrid action of DWF valence on staggered sea quarks, there is a nice agreement among different lattice discretizations and no significant dependence on the quark mass down to about $m_\pi = 270$ MeV.

We take the continuum limit of TMF results by fitting to a constant, after checking that a linear fit at two values of the pion mass yields consistent results with the constant fit. Volume corrections are taken into account following Ref. [3]. The volume corrected continuum results are shown in Fig. 1. Chiral extrapolation using HB χ PT with three fit parameters in the small scale expansion (SSE) [4] produces a value of $g_A = 1.12(8)$ at the physical point, which is lower than the experimental value by about a standard deviation. The large error band is due to the large

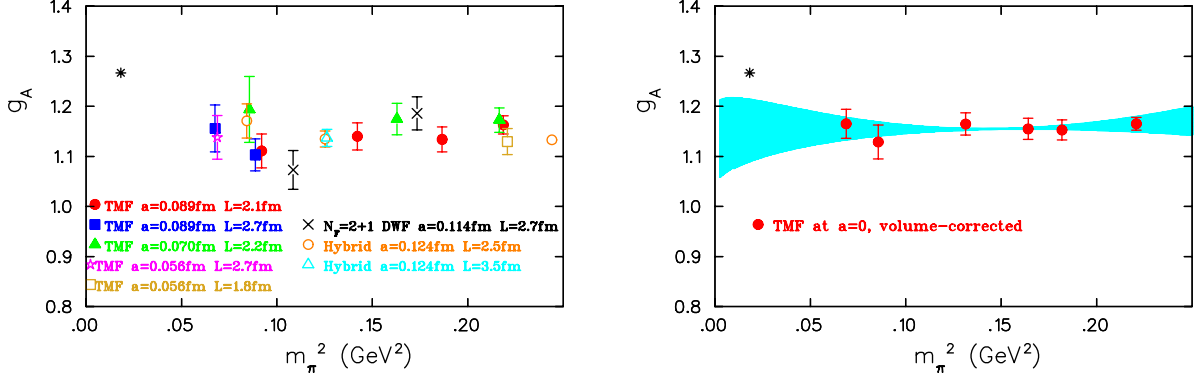


Figure 1: Left: Lattice data on g_A using $N_F = 2$ TMF [1], $N_F = 2 + 1$ DWF [5] and $N_F = 2 + 1$ using DWF on staggered sea quarks [6]. The physical point is shown by the asterisk. Right: Volume corrected continuum TMF results together with the band obtained using HB χ PT.

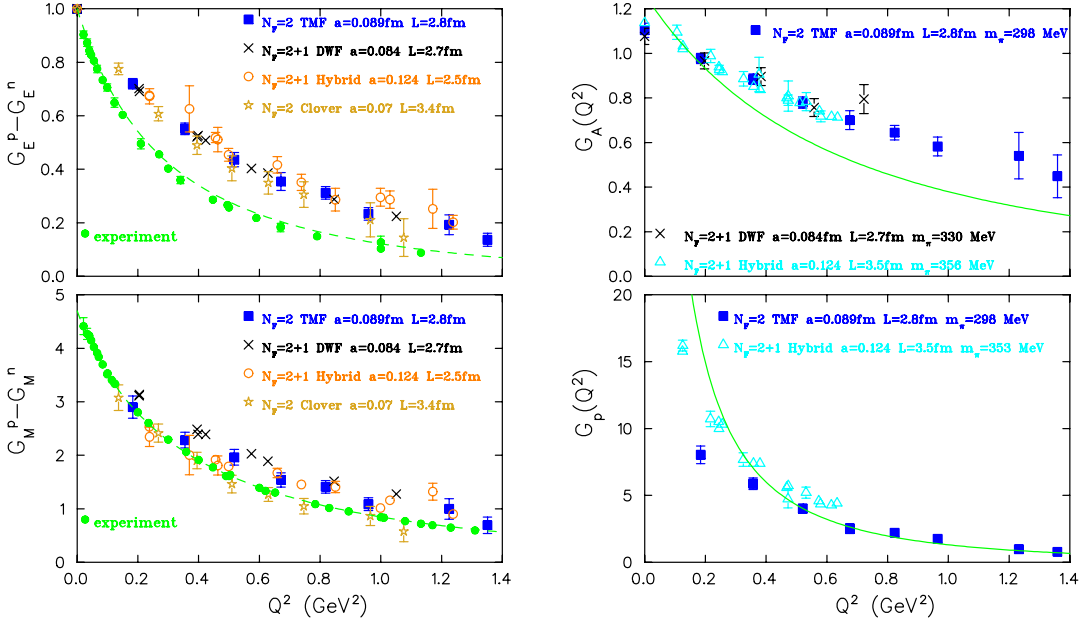


Figure 2: Left: Isovector electric and magnetic nucleon FFs at $m_\pi \sim 300$ MeV using TMF [1], DWF [7], hybrid [6] and Clover [8]. Experimental data are shown with the filled circles accompanied with Kelly's parametrization shown with the dashed line. Right: Axial nucleon FFs. The solid line is a dipole fit to experimental data for $G_A(Q^2)$ combined with pion pole dominance to get the solid curve shown for $G_p(Q^2)$.

correlations between the Δ axial charge $g_{\Delta\Delta}$ and the counter-term involved in the chiral expansion. A lattice determination of $g_{\Delta\Delta}$ [9] will therefore allow a more controlled chiral extrapolation.

In Fig. 2 we show recent lattice results on the EM isovector FFs $G_E(Q^2)$ and $G_M(Q^2)$ at $m_\pi \sim 300$ MeV, where we see a nice agreement for $G_E(Q^2)$ but a clear disagreement with experiment, with lattice data showing a weaker Q^2 -dependence. For $G_M(Q^2)$ there is some spread in the results that needs to be investigated. For the axial $G_A(Q^2)$ FF there is good agreement among TMF, DWF and hybrid results. Like in the case of the EM form factors, the Q^2 -dependence of $G_A(Q^2)$ is milder than what is observed experimentally. TMF results on $G_p(Q^2)$ at $m_\pi \sim 300$ MeV on a lattice with

spatial $L = 2.8$ fm and results using a hybrid action of DWF on staggered sea at $m_\pi \sim 350$ MeV and $L = 3.5$ fm show discrepancies at low Q^2 , that may be due to the smaller volume in our calculations.

3. Nucleon moments

In Figs. 3 we compare recent results from ETMC [1], RBC-UKQCD [10], QCDSF [11] and LHPC [6] on the spin-independent and helicity quark distributions. All collaborations except LHPC use non-perturbative renormalization constants. The ETMC has, in addition, subtracted $\mathcal{O}(a^2)$ terms perturbatively [2]. There is a spread among lattice results with results obtained with the hybrid action being lower than those from ETMC and QCDSF. Using HB χ PT [12] we extrapolate results on A_{20} and \tilde{A}_{20} to the physical point as shown by the curves in Fig. 3. Our estimates for both $A_{20} = \langle x \rangle_{u-d}$ and $\tilde{A}_{20} = \langle x \rangle_{\Delta u - \Delta d}$ are considerably higher than the experimental values. The very recent result by QCDSF [11] at $m_\pi \sim 170$ MeV remains higher than experiment and highlights the need to understand such deviations.

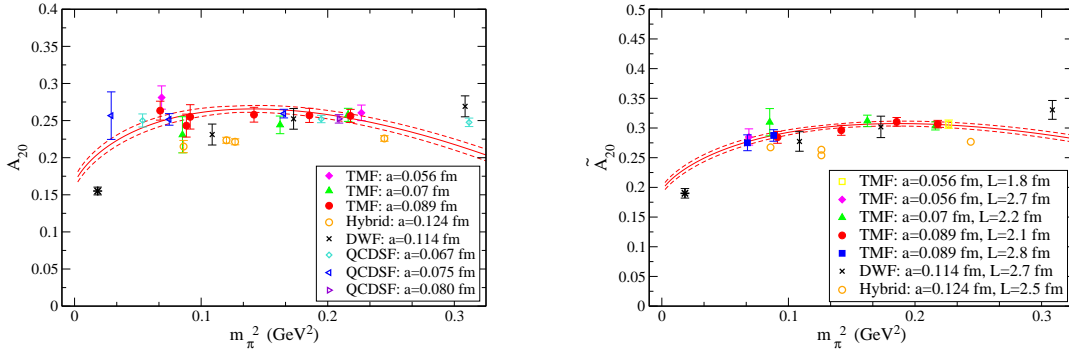


Figure 3: Recent results on $\langle x \rangle_{u-d}$ and $\langle x \rangle_{\Delta u - \Delta d}$. The fit is done using HB χ PT [12].

References

- [1] C. Alexandrou, PoS **Lattice 2010**, 001 (2010), arXiv:1011.3660; C. Alexandrou *et al.*, (ETMC) PoS **LATTICE2008**, 139 (2008); C. Alexandrou *et al.* (ETMC), PoS **LAT2009** 145 (2009).
- [2] C. Alexandrou, M. Constantinou, T. Korzec, H. Panagopoulos and F. Stylianou, arXiv:1006.1920.
- [3] A. Ali Khan, *et al.* (QCDSF), PRD **74**, 094508 (2006).
- [4] T. R. Hemmert, M. Procura and W. Weise, Phys. Rev. D **68**, 075009 (2003).
- [5] T. Yamazaki *et al.* (RBC-UKQCD), PRD **79**, 14505 (2009).
- [6] J. D. Bratt *et al.* (LHPC), arXiv:1001.3620.
- [7] S. N. Syritsyn *et al.* (LHPC), Phys. Rev. D **81**, 034507 (2010).
- [8] S. Capitani, M. Della Morte, B. Knippschild and H. Wittig, arXiv:1011.1358.
- [9] C. Alexandrou *et al.*, arXiv:1011.0411 [hep-lat].
- [10] Y. Aoki *et al.*, (RBC-UKQCD), Phys. Rev. D **79**, 114505 (2009).
- [11] J. Zanotti (QCDSF), private communication.
- [12] D. Arndt, M. Savage, Nucl. Phys. A **697**, 429 (2002); W. Detmold, W. Melnitchouk, A. Thomas, Phys. Rev. D **66**, 054501 (2002).